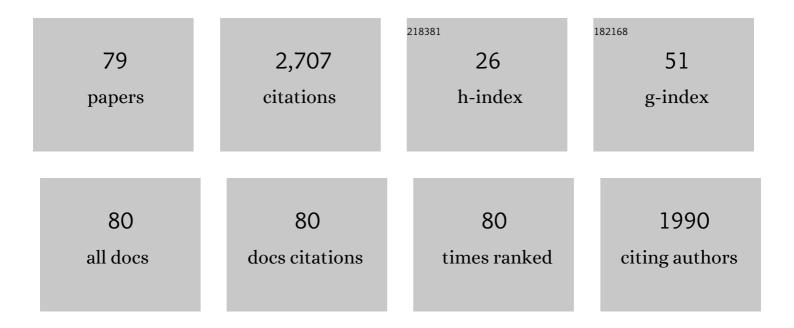
List of Publications by Year in descending order

Source: https://exaly.com/author-pdf/4482059/publications.pdf Version: 2024-02-01



#	Article	IF	CITATIONS
1	Quantification of myocardial blood flow with 82Rb dynamic PET imaging. European Journal of Nuclear Medicine and Molecular Imaging, 2007, 34, 1765-1774.	3.3	373
2	Does quantification of myocardial flow reserve using rubidium-82 positron emission tomography facilitate detection of multivessel coronary artery disease?. Journal of Nuclear Cardiology, 2012, 19, 670-680.	1.4	252
3	Machine Learning and Deep Learning in Medical Imaging: Intelligent Imaging. Journal of Medical Imaging and Radiation Sciences, 2019, 50, 477-487.	0.2	217
4	Quantification of myocardial blood flow and flow reserve: Technical aspects. Journal of Nuclear Cardiology, 2010, 17, 555-570.	1.4	149
5	Quantification of Myocardial Blood Flow inÂAbsolute Terms Using 82Rb PET Imaging. JACC: Cardiovascular Imaging, 2014, 7, 1119-1127.	2.3	144
6	Dynamic SPECT Measurement of Absolute Myocardial Blood Flow in a Porcine Model. Journal of Nuclear Medicine, 2014, 55, 1685-1691.	2.8	134
7	Intra- and inter-operator repeatability of myocardial blood flow and myocardial flow reserve measurements using rubidium-82 pet and a highly automated analysis program. Journal of Nuclear Cardiology, 2010, 17, 600-616.	1.4	126
8	Multisoftware Reproducibility Study of Stress and Rest Myocardial Blood Flow Assessed with 3D Dynamic PET/CT and a 1-Tissue-Compartment Model of ⁸² Rb Kinetics. Journal of Nuclear Medicine, 2013, 54, 571-577.	2.8	110
9	Is There an Association Between Clinical Presentation and the Location and Extent of Myocardial Involvement of Cardiac Sarcoidosis as Assessed by ¹⁸ F- Fluorodoexyglucose Positron Emission Tomography?. Circulation: Cardiovascular Imaging, 2013, 6, 617-626.	1.3	83
10	Absolute myocardial flow quantification with 82Rb PET/CT: comparison of different software packages and methods. European Journal of Nuclear Medicine and Molecular Imaging, 2014, 41, 126-135.	3.3	77
11	Comparison of 18F-fluorodeoxyglucose positron emission tomography (FDG PET) and cardiac magnetic resonance (CMR) in corticosteroid-naive patients with conduction system disease due to cardiac sarcoidosis. European Journal of Nuclear Medicine and Molecular Imaging, 2016, 43, 259-269.	3.3	73
12	Short-term repeatability of resting myocardial blood flow measurements using rubidium-82 PET imaging. Journal of Nuclear Cardiology, 2012, 19, 997-1006.	1.4	68
13	Patient motion effects on the quantification of regional myocardial blood flow with dynamic PET imaging. Medical Physics, 2016, 43, 1829-1840.	1.6	68
14	Generator-produced rubidium-82 positron emission tomography myocardial perfusion imaging—From basic aspects to clinical applications. Journal of Cardiology, 2010, 55, 163-173.	0.8	57
15	Feasibility and operator variability of myocardial blood flow and reserve measurements with 99mTc-sestamibi quantitative dynamic SPECT/CT imaging. Journal of Nuclear Cardiology, 2014, 21, 1075-1088.	1.4	54
16	Incremental Diagnostic Value of Regional Myocardial Blood Flow Quantification Over Relative Perfusion Imaging With Generator-Produced Rubidium-82 PET. Circulation Journal, 2011, 75, 2628-2634.	0.7	50
17	Consistent tracer administration profile improves test–retest repeatability of myocardial blood flow quantification with 82Rb dynamic PET imaging. Journal of Nuclear Cardiology, 2018, 25, 929-941.	1.4	45
18	Angiotensin Receptor Neprilysin Inhibitor Attenuates Myocardial Remodeling and Improves Infarct Perfusion in Experimental Heart Failure. Scientific Reports, 2019, 9, 5791.	1.6	43

#	Article	IF	CITATIONS
19	PET and SPECT Tracers for Myocardial Perfusion Imaging. Seminars in Nuclear Medicine, 2020, 50, 208-218.	2.5	39
20	Quantitative analysis of coronary endothelial function with generator-produced 82Rb PET: comparison with 150-labelled water PET. European Journal of Nuclear Medicine and Molecular Imaging, 2010, 37, 2233-2241.	3.3	35
21	Repeatable Noninvasive Measurement of Mouse Myocardial Glucose Uptake with ¹⁸ F-FDG: Evaluation of Tracer Kinetics in a Type 1 Diabetes Model. Journal of Nuclear Medicine, 2013, 54, 1637-1644.	2.8	35
22	Inter- and Intraobserver Agreement of ¹⁸ F-FDG PET/CT Image Interpretation in Patients Referred for Assessment of Cardiac Sarcoidosis. Journal of Nuclear Medicine, 2017, 58, 1324-1329.	2.8	32
23	Quantification of regional myocardial blood flow estimation with three-dimensional dynamic rubidium-82 PET and modified spillover correction model. Journal of Nuclear Cardiology, 2012, 19, 763-774.	1.4	31
24	Myocardial blood flow quantification by Rb-82 cardiac PET/CT: A detailed reproducibility study between two semi-automatic analysis programs. Journal of Nuclear Cardiology, 2016, 23, 499-510.	1.4	29
25	Test–retest repeatability of quantitative cardiac 11C-meta-hydroxyephedrine measurements in rats by small animal positron emission tomography. Nuclear Medicine and Biology, 2013, 40, 676-681.	0.3	28
26	Cardiac CT assessment of left ventricular mass in mid-diastasis and its prognostic value. European Heart Journal Cardiovascular Imaging, 2017, 18, 95-102.	0.5	27
27	Diastolic dysfunction can precede systolic dysfunction on MUGA in cancer patients receiving trastuzumab-based therapy. Nuclear Medicine Communications, 2019, 40, 22-29.	0.5	20
28	Effects of Hypercapnia on Myocardial Blood Flow in Healthy Human Subjects. Journal of Nuclear Medicine, 2018, 59, 100-106.	2.8	18
29	Application of Hybrid Matrix Metalloproteinase-Targeted and Dynamic ²⁰¹ Tl Single-Photon Emission Computed Tomography/Computed Tomography Imaging for Evaluation of Early Post-Myocardial Infarction Remodeling. Circulation: Cardiovascular Imaging, 2019, 12, e009055.	1.3	18
30	Respiratory phase alignment improves blood-flow quantification in Rb82 PET myocardial perfusion imaging. Medical Physics, 2013, 40, 022503.	1.6	16
31	Radionuclide Tracers for Myocardial Perfusion Imaging and Blood Flow Quantification. Cardiology Clinics, 2016, 34, 37-46.	0.9	15
32	Validation of a Multimodality Flow Phantom and Its Application for Assessment of Dynamic SPECT and PET Technologies. IEEE Transactions on Medical Imaging, 2017, 36, 132-141.	5.4	14
33	Quantitative blood flow evaluation of vasodilation-stress compared with dobutamine-stress in patients with end-stage liver disease using 82Rb PET/CT. Journal of Nuclear Cardiology, 2020, 27, 2048-2059.	1.4	12
34	Quantification of regional myocardial blood flow in a canine model of stunned and infarcted myocardium: comparison of rubidium-82 positron emission tomography with microspheres. Nuclear Medicine Communications, 2010, 31, 67-74.	0.5	11
35	Uniformity and repeatability of normal resting myocardial blood flow in rats using [13N]-ammonia and small animal PET. Nuclear Medicine Communications, 2012, 33, 917-925.	0.5	11
36	Rubidium-82 generator yield and efficiency for PET perfusion imaging: Comparison of two clinical systems. Journal of Nuclear Cardiology, 2020, 27, 1728-1738.	1.4	11

#	Article	IF	CITATIONS
37	Preclinical Evaluation of Biopolymer-Delivered Circulating Angiogenic Cells in a Swine Model of Hibernating Myocardium. Circulation: Cardiovascular Imaging, 2013, 6, 982-991.	1.3	10
38	Reduced dose measurement of absolute myocardial blood flow using dynamic SPECT imaging in a porcine model. Medical Physics, 2015, 42, 5075-5083.	1.6	9
39	Reproducibility of radioactive iodine uptake (<scp>RAIU</scp>) measurements. Journal of Applied Clinical Medical Physics, 2018, 19, 239-242.	0.8	9
40	Accurate GFR in obesity—protocol for a systematic review. Systematic Reviews, 2019, 8, 147.	2.5	9
41	Test–retest repeatability of myocardial blood flow and infarct size using 11C-acetate micro-PET imaging in mice. European Journal of Nuclear Medicine and Molecular Imaging, 2015, 42, 1589-1600.	3.3	8
42	Optimally Repeatable Kinetic Model Variant for Myocardial Blood Flow Measurements with ⁸² Rb PET. Computational and Mathematical Methods in Medicine, 2017, 2017, 1-11.	0.7	8
43	Quantitative analysis of technetium-99m-sestamibi uptake and washout in parathyroid scintigraphy supports dual mechanisms of lesion conspicuity. Nuclear Medicine Communications, 2019, 40, 469-476.	0.5	8
44	Selection of PET Camera and Implications on the Reliability and Accuracy of Absolute Myocardial Blood Flow Quantification. Current Cardiology Reports, 2020, 22, 109.	1.3	8
45	Increased myocardial oxygen consumption rates are associated with maladaptive right ventricular remodeling and decreased event-free survival in heart failure patients. Journal of Nuclear Cardiology, 2021, 28, 2784-2795.	1.4	8
46	Clinical comparison of the positron emission tracking (PeTrack) algorithm with the realâ€ŧime position management system for respiratory gating in cardiac positron emission tomography. Medical Physics, 2020, 47, 1713-1726.	1.6	8
47	3D versus 2D dynamic 82Rb myocardial blood flow imaging in a canine model of stunned and infarcted myocardium. Nuclear Medicine Communications, 2010, 31, 75-81.	0.5	7
48	Detection and severity classification of extracardiac interference in ⁸² Rb PET myocardial perfusion imaging. Medical Physics, 2014, 41, 102501.	1.6	7
49	3D list-mode cardiac PET for simultaneous quantification of myocardial blood flow and ventricular function. , 2008, , .		6
50	β2-adrenergic stress evaluation of coronary endothelial-dependent vasodilator function in mice using 11C-acetate micro-PET imaging of myocardial blood flow and oxidative metabolism. EJNMMI Research, 2014, 4, 68.	1.1	6
51	82Rb PET imaging of myocardial blood flow—have we achieved the 4 "Râ€s to support routine use?. EJNMMI Research, 2016, 6, 69.	1.1	6
52	Time-frame sampling for 82Rb PET flow quantification: Towards standardization of clinical protocols. Journal of Nuclear Cardiology, 2017, 24, 1530-1534.	1.4	6
53	Dual time-point quantitative SPECT-CT parathyroid imaging using a single computed tomography. Nuclear Medicine Communications, 2018, 39, 3-9.	0.5	6
54	Patient body motion correction for dynamic cardiac <scp>PET</scp> â€ <scp>CT</scp> by attenuationâ€emission alignment according to projection consistency conditions. Medical Physics, 2019, 46, 1697-1706.	1.6	6

<u> </u>		
Ran	KIE	ΊN
	NLL	шı

#	Article	IF	CITATIONS
55	Anatomical region identification in medical X-ray computed tomography (CT) scans: development and comparison of alternative data analysis and vision-based methods. Neural Computing and Applications, 2020, 32, 17519-17531.	3.2	5
56	Intensity of hypermetabolic axillary lymph nodes in oncologic patients in relation to timeline following COVID-19 vaccination. Journal of Medical Imaging and Radiation Sciences, 2022, , .	0.2	5
57	Constant-Activity-Rate Infusions for Myocardial Blood Flow Quantification with 82Rb and 3D PET. , 2006, , .		4
58	Can PET be performed without an attenuation scan?. Journal of Nuclear Cardiology, 2016, 23, 1098-1101.	1.4	4
59	⁸² Rb is the Best Flow Tracer for High-volume Sites. Annals of Nuclear Cardiology, 2019, 5, 53-62.	0.0	4
60	Guidelines on Setting Up Stations for Remote Viewing of Nuclear Medicine and Molecular Imaging Studies During COVID-19. Journal of Nuclear Medicine Technology, 2021, 49, 2-6.	0.4	4
61	Evaluation of the clinical efficacy of the PeTrack motion tracking system for respiratory gating in cardiac PET imaging. Proceedings of SPIE, 2017, , .	0.8	3
62	Development and validation of the Lesion Synthesis Toolbox and the Perception Study Tool for quantifying observer limits of detection of lesions in positron emission tomography. Journal of Medical Imaging, 2020, 7, 1.	0.8	3
63	Positron Emission Tomography Myocardial Perfusion Imaging for Diagnosis and Risk Stratification in Obese Patients. Current Cardiovascular Imaging Reports, 2015, 8, 1.	0.4	2
64	Editorial: Derivation of respiratory gating signals from ECG signals. Journal of Nuclear Cardiology, 2016, 23, 84-86.	1.4	2
65	Whole-body motion correction in cardiac PET/CT using Positron Emission Tracking: A phantom validation study. , 2018, , .		2
66	An electronic technetium-99m-diethylenetriaminepentaacetic acid glomerular filtration rate spreadsheet with novel embedded quality assurance features. Nuclear Medicine Communications, 2019, 40, 30-40.	0.5	2
67	Initial Steps to Tracer Kinetic Modeling and MBF Quantification. Annals of Nuclear Cardiology, 2018, 4, 68-73.	0.0	2
68	Validation of regional myocardial blood flow quantification using three-dimensional PET with rubidium-82: repeatability and comparison with two-dimensional PET data acquisition. Nuclear Medicine Communications, 2020, 41, 768-775.	0.5	1
69	Dynamic phantoms: Making the right tool for the job. Journal of Nuclear Cardiology, 2021, 28, 2310-2312.	1.4	1
70	Keiichiro Yoshinaga, MD, PhD, FACC, FASNC. Journal of Nuclear Cardiology, 2021, 28, 377-380.	1.4	1
71	Cardiac PET Imaging: Principles and New Developments. , 2017, , 451-483.		1
72	Developing an Automatic Cooperating Neural Networks and Image Standardization Approach for Segmentation of X-Ray Computed Tomography Images. Advances in Intelligent Systems and Computing, 2021, , 390-401.	0.5	1

#	Article	IF	CITATIONS
73	Reply: Noninvasive Measurement of Mouse Myocardial Glucose Uptake with ¹⁸ F-FDG. Journal of Nuclear Medicine, 2014, 55, 866.2-867.	2.8	0
74	Whole-body motion correction in 13N-ammonia myocardial perfusion imaging using positron emission tracking. , 2019, , .		0
75	Use of Radiolabeled Compounds and Imaging as Cardiac Biomarkers. , 2014, , 1-23.		0
76	Use of Radiolabeled Compounds and Imaging as Cardiac Biomarkers. Biomarkers in Disease, 2015, , 811-840.	0.0	0
77	Sci-Fri AM: MRI and Diagnostic Imaging - 05: Comparison of Input Function Measurements from DCE and MOLLI. Medical Physics, 2016, 43, 4952-4952.	1.6	0
78	Does Diastolic Dysfunction Precede Systolic Dysfunction Following Contemporary Breast Cancer Therapy?. JACC: Cardiovascular Imaging, 2020, 13, 1454-1455.	2.3	0
79	Thyroid Uptake Exceeding 100%: Causes and Prevention. Journal of Nuclear Medicine Technology, 2022, 50, 153-160.	0.4	0